Nanotechnology **20** (2009) 095702 (6pp) doi:10.1088/0957-4484/20/9/095702

The influence of local heating by nonlinear pulsed laser excitation on the transmission characteristics of a ZnO nanowire waveguide

Tobias Voss[1,2,5], Geoffry T Svacha[1,2], Eric Mazur[1,2], Sven Müller[3] and Carsten Ronning[4]

[1] Department of Physics, Harvard University, 9 Oxford Street, Cambridge, MA 02138, USA
[2] School of Engineering and Applied Sciences, Harvard University, 9 Oxford Street, Cambridge, MA 02138, USA
[3] II. Physikalisches Institut, University of Göttingen, Göttingen, Germany
[4] Institute of Solid State Physics, University of Jena, Jena, Germany

Received 24 October 2008, in final form 27 October 2008
Published 11 February 2009
Online at stacks.iop.org/Nano/20/095702

Abstract
We perform a transmission experiment on a ZnO nanowire waveguide to study its transmission characteristics under nonlinear femtosecond-pulse excitation. We find that both the second harmonic and the photoluminescence couple into low-order waveguide modes of the nanowires but with distinctly different efficiencies. We measure the transmission spectrum of a single ZnO nanowire waveguide for near-UV light generated by interband recombination processes. The transmission spectrum allows us to determine the absorption edge of the excited nanowire and to study the temperature profile of the nanowire under femtosecond-pulse excitation.

(Some figures in this article are in colour only in the electronic version)

1. Introduction

Zinc oxide (ZnO) is a non-toxic, wide-band gap semiconductor used in electronic and near-UV optoelectronic devices such as sensors, light emitters and detectors [1, 2]. ZnO has received much attention because it is easy to fabricate large quantities of high-quality ZnO nanowires with diameters of a few hundred nanometers and lengths of several tens of micrometers [3–6]. Such nanowires are transparent throughout the visible spectral region, due to the large room temperature band gap $E_{gap} = 3.37$ eV of ZnO [1, 7]. Furthermore, because of the large refractive index of ZnO across the visible spectrum ($n > 2$) [7], ZnO nanowires are excellent low-loss sub-wavelength waveguides. The large index provides tight optical confinement for low-order modes and also results in a large acceptance angle for coupling light into the nanowire waveguide. Although the hexagonal cross-section of the nanowires influences the intensity profile of higher-order modes, the lowest-order mode exhibits almost circular symmetry inside the nanowire [8]. The semiconducting properties of the material permit the fabrication of nanowire devices [3, 4, 9–11] in which gain and refractive index can be electrically modulated. However, efficient and reliable p-type doping of ZnO remains an unsolved problem hindering the design of electrically operated nanowire devices [2].

Because ZnO is a highly polar semiconductor it is frequently used for frequency doubling of intense ultrashort laser pulses [12]. Several studies report on the nonlinear coefficients [12–16] of *c*-plane and *a*-plane ZnO thin films, and on second-harmonic generation [17] and polariton effects [18] in ZnO nanowires.

In this work, we show that nonlinear excitation of individual ZnO nanowires with ultrashort laser pulses excites waveguide modes in the nanowires. We study the coupling and transmission efficiency of the photoluminescence and second-harmonic generation in the nanowire. We perform transmission measurements on a single nanowire and determine the absorption edge of the highly excited semiconductor material. The absorption edge allows us to deduce an upper limit for the local temperature of the nanowire close to the excitation spot.

[5] Present address: Institute of Solid State Physics, University of Bremen, Bremen, Germany.

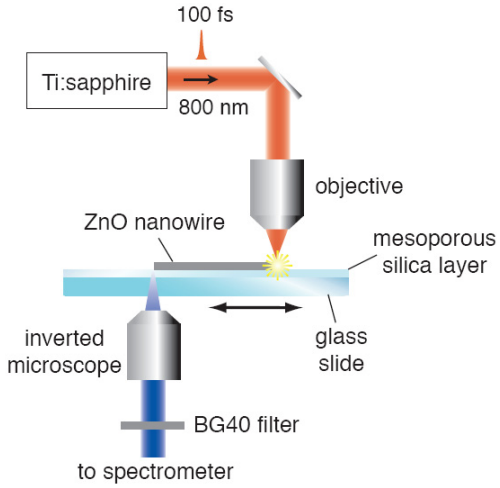

Figure 1. Experimental setup. A ZnO nanowire is lying on a glass slide covered with a 800 nm layer of low-index mesoporous silica. The nanowire is excited from the top perpendicular to its *c*-axis. The emission from the nanowire is observed with an inverted microscope.

We perform finite-element simulations to model the heat distribution of a ZnO nanowire under excitation with intense femtosecond laser pulses.

2. Experimental details

We grow ZnO nanowires by a vapor transport technique using high-purity ZnO powder as source material [5]. The ZnO powder is heated up to 1620 K in a horizontal tube furnace, and a constant flow of Ar gas transports the ZnO vapor through the furnace. Large quantities of *c*-axis oriented nanowires grow on silicon substrates covered with 4 nm thin Au films that are placed in a cooler region of the furnace where the temperature is about 1380 K. We mechanically disperse the nanowires onto glass slides that are covered with 800 nm thick films of mesoporous silica. This method yields mesoporous silica substrates covered with nanowires of 20–60 μm length, 200–400 nm diameter, and a separation between the nanowires that is large enough to study single nanowires.

The mesoporous silica films consist of 8 nm wide pores filled with air resulting in a low refractive index of $n = 1.185$ throughout the whole visible spectrum [19, 20]. The low refractive index, the homogeneity, and the flatness of the mesoporous silica minimize the waveguiding losses in the ZnO nanowires and prevent parasitic scattering and coupling into the substrate because of the large index contrast $\Delta n = 0.8$ between the nanowire waveguide and the mesoporous silica layer.

We performed the experiments described in this paper using an inverted microscope, shown schematically in figure 1. The nanowires are excited from the top with the fundamental 800 nm pulses from a femtosecond laser oscillator (60 fs; 11 MHz; 80 nJ). The incident radiation is normal to the waveguide direction of the nanowires. A reflection type objective (40×; 0.5 NA) focuses the laser pulses onto the nanowires to a spot size with a diameter <10 μm. We estimate the typical excitation fluence at the excitation spot to be 0.45 kJ m^{-2}, well below the damage threshold for ZnO nanowires which we determined to be about 5–10 times higher. Using a fiber-coupled spectrometer we spatially resolve the emission spectrum of the nanowire at the image plane of an output port of the microscope. A BG40 color-glass filter attenuates the 800 nm signal from the excitation pulses while providing high and nearly constant transmission over the entire ZnO emission spectrum (transmission between 0.85 and 0.90 between 350 and 550 nm).

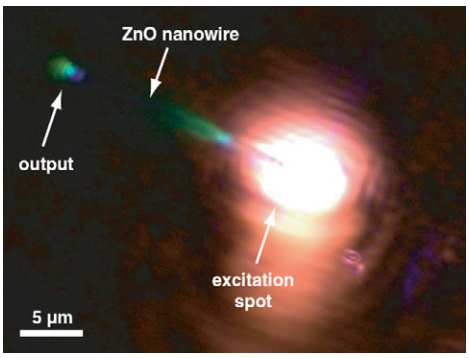

Figure 2. Microscope image of a single ZnO nanowire under infrared femtosecond-pulse excitation. Near the excitation spot residual infrared light, blue and green photoluminescence, and second-harmonic light can be observed. The far end of the nanowire shows emission of photoluminescence that is guided along the length of the nanowire without visible waveguiding losses.

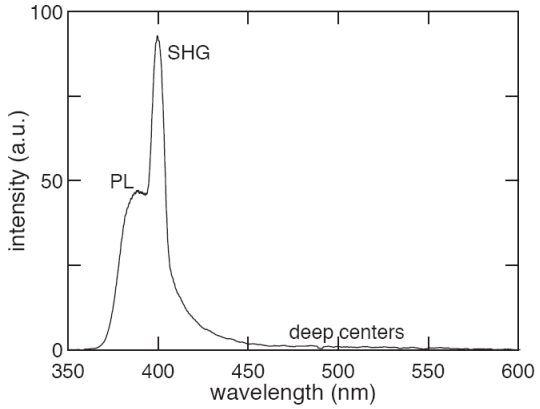

Figure 3. Spectrum of the light collected directly at the excitation spot of a single nanowire irradiated by 800 nm fs pulses. The second harmonic (SHG) of the laser line is clearly visible at 400 nm on top of a photoluminescence (PL) pedestal ranging from 370 to 450 nm. Between 475 and 575 nm we find weak green emission from deep centers.

3. Results

Figure 2 shows a microscope image of a ZnO nanowire excited at one end with 800 nm fs pulses. In spite of the BG40 filter, residual red light is still clearly visible around the excitation spot. Close to the excitation spot, we observe blue and green emission. Figure 3 shows a spectrum of the emission. In addition to a pronounced second-harmonic peak

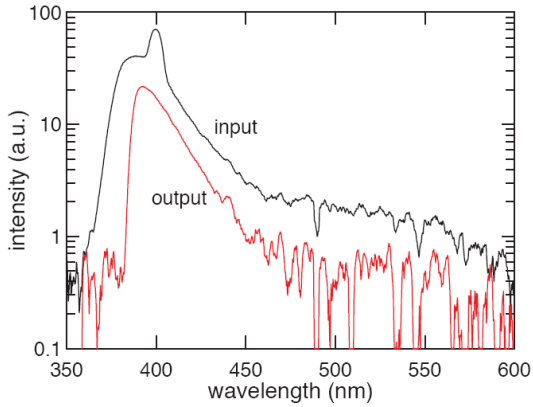

Figure 4. Emission spectrum of a single nanowire at the excitation spot (input) and spectrum of the light emitted at the other end of the nanowire 25 μm away from the excitation spot (output).

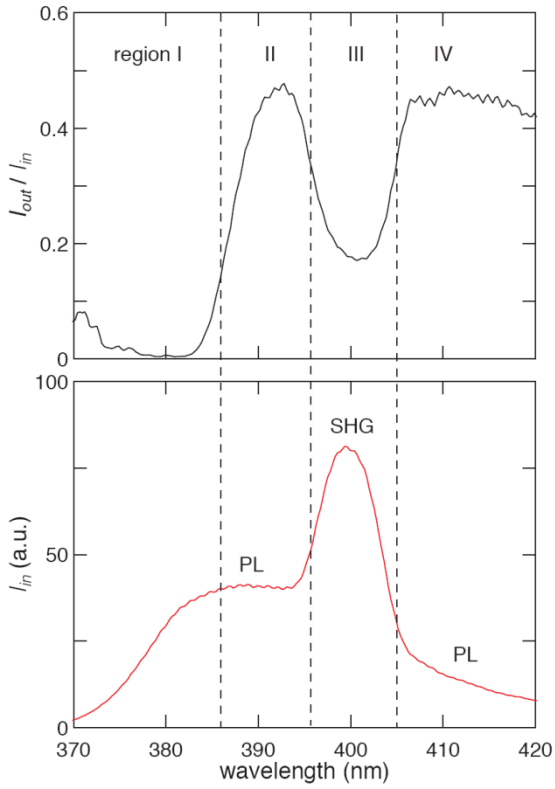

Figure 5. Ratio of output to input intensity for a single nanowire. The input spectrum is also shown for comparison. The spectra are divided into four regions discussed in the text.

at 400 nm, the spectrum shows photoluminescence from near band-edge recombination [2] located at 387 nm, most probably originating from a Coulomb-correlated electron–hole plasma and from deep centers in the ZnO nanowires centered around 500 nm [2]. Compared to the photoluminescence measured with a cw HeCd-laser at wavelength of 325 nm, the main photoluminescence peak is slightly red-shifted by about $\Delta\lambda = 2$ nm. Figure 2 also shows that part of the photoluminescence and second harmonic of the excitation pulses is guided to the far end of the nanowire where we can clearly see the blue and green components of the emission from the waveguide mode. Apart from the regions directly around the excitation spot and at the far end of the nanowire, no further emission from the nanowire waveguide is visible.

Figure 4 compares the spectra measured directly at the excitation spot (input) and at the far end of the nanowire, 25 μm away from the excitation spot (output). As expected, the output intensity is distinctly weaker than the input intensity. The peak due to second-harmonic generation is absent in the output spectrum. In the spectral range below 390 nm, the output intensity drops sharply to the noise level, even though the input intensity is still significant. At long wavelengths, the output spectrum follows the same general trend as the input spectrum.

To understand the relation between the two spectra in figure 4, we plot their ratio $I_{\text{out}}/I_{\text{in}}$ in figure 5. For comparison we also show the input spectrum, on a linear scale. The ratio $I_{\text{out}}/I_{\text{in}}$ in figure 5 can be interpreted as a transmission spectrum that also accounts for the different coupling efficiencies of the photoluminescence and second-harmonic generation into the waveguide modes of the nanowire waveguide. We can identify four different regions in this transmission spectrum. In region I the $I_{\text{out}}/I_{\text{in}}$ is close to zero even though we observe considerable intensity in the corresponding part of the input spectrum. In region II the photoluminescence in the input spectrum is maximum and $I_{\text{out}}/I_{\text{in}}$ has a local maximum. Region III, which is at the position of the second harmonic in the input spectrum, shows a decrease in $I_{\text{out}}/I_{\text{in}}$. In region IV $I_{\text{out}}/I_{\text{in}}$ increases again to the same approximately constant value as in region II and the input spectrum shows contributions from the photoluminescence.

In figure 6, we show the results of 3D finite-element simulations of the temperature distribution in a hexagonal ZnO nanowire. The nanowire with a length of 15 μm and a diameter of 200 nm (measured from edge to edge of the hexagon) is lying on a glass substrate covered with a 1 μm thick layer of mesoporous silica. The ratios of the thermal conductivities $c_{\text{ZnO}}/c_{\text{mesoporous\_silica}}/c_{\text{glass}}/c_{\text{air}}$ are taken as 10/0.1/1/0.02 [25, 26]. The value c_{ZnO} considers the reduced thermal conductivity nanostructures compared to the standard bulk values by about a factor of 10 [25]. At one of its ends, the nanowire is heated up to a temperature of 600 K by applying a constant heat source in the simulation (modeled by a 2 μm long internally heated additional piece of nanowire added to the passive nanowire).

We obtain the results shown in figure 6 by numerically solving the heat-conductivity equation for the system with the computer program FlexPDE. The computational cell extends from -450 to $+450$ μm in the x- and y-directions, and from -15 to $+15$ μm in z-direction. The boundaries are kept constant at room temperature $T = 300$ K. The nanowire is centered at the origin of the computational cell. The heated nanowire piece is located in the region between $x = 7.5$ and 9.5 μm. Figure 6(a) represents the two-dimensional temperature profiles in the region of the nanowire in the x–y plane at $z = 0$ μm and the x–z plane at $y = 0$ μm, respectively. In figure 6(b) we show the temperature profile

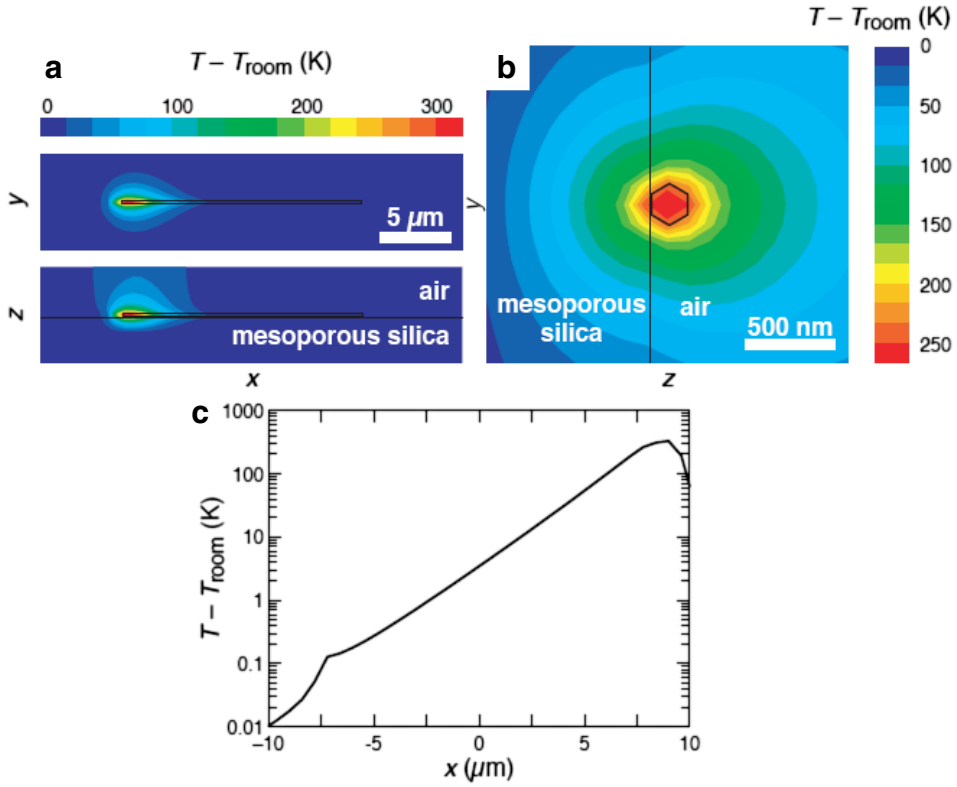

Figure 6. Finite-element simulations of the temperature profiles of a locally heated ZnO nanowire lying on a glass substrate that is covered with a layer of mesoporous silica. (a) 2D temperature profiles in the x–y and x–z planes for $z = 0$ μm and $y = 0$ μm, respectively. (b) Temperature profile in the z–y plane for $x = 7.5$ μm. (c) Temperature increase $T - T_{\text{room}}$ as a function of x for $y = 0$ μm, $z = 0$ μm plotted on a logarithmic scale.

in the y–z plane at $x = 7.5$ μm (adjacent to the heated region $x = 7.5$–9.5 μm). The one-dimensional temperature increase $T - T_{\text{room}}$ along the x-direction of the nanowire is plotted in figure 6(c) for $y = 0$ μm, $z = 0$ μm. The simulations demonstrate an almost strictly monoexponential decay of the temperature difference $T - T_{\text{room}}$ along the nanowire. With the constants used in the simulation, we find in figure 6(c) a characteristic length scale of about 3.5 μm after which $T - T_{\text{room}}$ has decreased by a factor of 10.

4. Discussion

Figures 2 and 3 show that it is possible to efficiently excite near band-edge photoluminescence and second-harmonic radiation in ZnO nanowires using 800 nm femtosecond laser pulses incident normal to the nanowires. Radiation incident normal to the c-plane of ZnO leads to a vanishing contribution from $\chi^{(2)}$ [12], but radiation normal to the a-plane of microcrystalline ZnO layers was shown to be especially favorable for second-harmonic generation [16]. Our results confirm that for nanowires, too, excitation normal to the side surfaces leads to efficient second-harmonic generation. In contrast to previously published results [17, 18], however, we observe only weak deep-level emission because of the high crystalline quality of our high-temperature grown nanowires.

Figures 4 and 5 show that the different contributions of the nonlinear nanowire emission couple into the waveguide modes of the nanowire with distinctly different efficiency. The minimum in the transmission spectrum in region III of figure 5 at the spectral position of the second-harmonic emission can be explained by the directed nature of the second-harmonic generation process. Because the nanowire is excited perpendicular to its waveguiding direction, the second harmonic of the excitation pulses is also preferentially emitted perpendicular to the waveguide. The large acceptance angle of the ZnO nanowires (about 40°, measured with respect to the symmetry axis of the waveguide) [21], however, still permits part of the second harmonic to couple into waveguide modes, albeit with a distinctly lower efficiency than the isotropically emitted photoluminescence. This lower coupling efficiency explains the decrease in $I_{\text{out}}/I_{\text{in}}$ at the second-harmonic wavelength in region III of figure 5.

The small value of in $I_{\text{out}}/I_{\text{in}}$ in region I of figure 5 can be attributed to re-absorption of the photoluminescence as it is guided along the nanowire. Under high-excitation conditions photoluminescence emission lines in semiconductors are significantly broadened and shifted by heating, band gap renormalization, screening and state filling [22]. The short-wavelength photoluminescence is sufficiently energetic to induce transitions across the band gap and is therefore absorbed in the unexcited part of the nanowire. This interband absorption reduces the transmission to almost zero in region I in figure 5.

We expect excitation of the nanowire with an 11 MHz train of intense ultrashort laser pulses to heat the nanowire

substantially. In a highly excited semiconductor, an increase in temperature and screening both reduce the band gap [22, 23]. Indeed, the absorption edge in figure 5 at $\lambda = (385 \pm 5)$ nm, corresponding to a band gap energy $E_{gap} = (3.22 \pm 0.04)$ eV, is shifted down from the room temperature value of the ZnO band gap, $E_{gap} = 3.370$ eV, by an amount $\Delta E = (150 \pm 40)$ meV [2, 24]. The observed shift in the band edge in figure 5 thus allows us to determine an upper limit for the temperature of the nanowire. In [27] we showed that the screening of the Coulomb interaction at high-excitation conditions (7 MW cm^{-2}, ns excitation-pulse duration) results in a red shift of the emission maximum of only 25 meV. We can therefore, in a first approximation, ignore the screening effects for the nonlinearly excited nanowires. Under this approximation, the results of [24] indicate that the band gap shift observed in our experiments corresponds to a temperature $T = (580 \pm 50)$ K of the ZnO nanowire, indicating a rise in temperature of about 300 K to a value that is still significantly below the melting temperature of the material.

The results of the finite-element simulation of the temperature distribution in figure 6 show that only the region 3 μm around the excitation spot is significantly heated. The still relatively high thermal conductivity of the nanowire material compared to that of air and substrate establishes the almost perfect monoexponential temperature decay along the nanowire. A few microns of nanowire material with a red-shifted band gap, however, are long enough for the waveguide modes to experience substantial absorption because typical absorption lengths in ZnO are around 300 nm. The numerical simulations therefore confirm that the local heating of nanowires under excitation with intense femtoseconds laser pulses can be quite substantial and presents an important consideration for the interpretation of corresponding experimental studies.

The high density of optically generated electron–hole pairs induces significant screening, band gap renormalization, and state filling at the excitation spot. All these effects cause a substantial broadening of the photoluminescence both toward lower and higher energies: state filling leads to the occupation of high-energy states, whereas the other effects reduce the energy of the emitted photons. Because of the short carrier diffusion length at room temperature (usually on the order of 100 nm) we expect a high carrier density only within the excitation spot. The large heat conductivity of the ZnO nanowire results in an increased temperature of the nanowire over a much longer length scale, as demonstrated by our numerical simulations: over more than 3 μm the temperature of the nanowires is substantially increased. This elevated temperature results in the re-absorption of the high-energy photons of the photoluminescence: the light is efficiently re-absorbed in the unexcited but still significantly heated part of the ZnO nanowire waveguide over a distance of a few micrometers away from the center of the excitation spot.

5. Conclusion

In summary, we generated blue and green photoluminescence and second-harmonic radiation by femtosecond multiphoton excitation of individual ZnO nanowires. We find that each of these contributions to the nonlinear nanowire emission couple into waveguide modes of the nanowire. By comparing the emission spectra at the input and output of the nanowire we can measure the transmission of a single nanowire. The resulting transmission spectra show that the photoluminescence and the second-harmonic couple into the waveguide modes with distinctly different efficiencies because the photoluminescence emission is isotropic, while the second-harmonic generation is mainly directed normal to the axis of the nanowire. The transmission spectra also show that the band gap of the excited nanowire is shifted to lower energy due to the elevated temperature of the nanowire at the excitation spot and due to screening effects in the highly excited nanowire. Our results reveal an upper limit for the temperature at the excitation spot of $T = (580 \pm 50)$ K under excitation with an 11 MHz pulse train of 60 fs pulses with an excitation fluence of 0.45 kJ m^{-2}. We have performed numerical simulations of the temperature distribution in a single ZnO nanowire that yield an almost monoexponentially decreasing temperature profile along the nanowire. The temperature increase is found to drop by one order of magnitude after a characteristic length of about 3.5 μm in the ZnO nanowire confirming the importance of local laser heating for the optical properties of these nanowires. Our results demonstrate that nonlinear femtoseconds-pulse excitation of semiconductor nanowires is a convenient method to study the transmission properties of individual nanowire waveguides. The same method will also be useful for analyzing the transmission characteristics of nanowire heterostructures and for studying the interaction of waveguide modes and their evanescent contributions with surrounding media.

Acknowledgments

Several people contributed to the work described in this paper. T Voss conceived the basic idea for this work, designed the experiment, and carried out the experiments. G T Svacha helped with the experiments and contributed to the development of the paper. C Ronning and S Müller fabricated and characterized the ZnO nanowires. E Mazur supervised the research and contributed to the development of the manuscript. T Voss wrote the first draft of the manuscript; all authors subsequently took part in the revision process. C R Mendonca and J Watkins provided feedback on the manuscript throughout its development. The mesoporous silica substrates were provided by D Konjhodzic and F Marlow, Max-Planck-Institut für Kohlenforschung, Mülheim, Germany. T Voss, C Ronning, and S Müller acknowledge funding from the German Research Foundation through grants VO1265/3, VO1265/4-1, and Ro1198/7-1,2. The research described in this paper is supported by the National Science Foundation under contracts PHY-0117795 and ECS-0601520. The authors would also like to acknowledge the use of facilities of the Center for Nanoscale Systems, which is supported by the National Science Foundation's National Nanotechnology Infrastructure Network. All experiments were carried out using a Femtosource Scientific XL laser.

References

[1] Look D C 2001 *Mater. Sci. Eng.* B **80** 383
[2] Klingshirn C, Hauschild R, Priller H, Decker M, Zeller J and Kalt H 2005 *Superlatt. Microstruct.* **38** 209
[3] Huang Y, Duan X and Lieber C M 2005 *Small* **1** 142
[4] Pauzauskie P J and Yang P 2006 *Mater. Today* **9** 36
[5] Borchers C, Müller S, Stichtenoth D, Schwen D and Ronning C 2006 *J. Phys. Chem.* B **110** 1656
[6] Wischmeier L, Voss T, Börner S and Schade W 2006 *Appl. Phys.* A **84** 111
[7] Yoshikawa H and Adachi S 1997 *Japan. J. Appl. Phys.* **36** 6237
[8] Hauschild R and Kalt H 2006 *Appl. Phys. Lett.* **89** 123107
[9] Bao J, Zimmler M A and Capasso F 2006 *Nano Lett.* **6** 1719
[10] Barrelet C J, Greytak A B and Lieber C M 2004 *Nano Lett.* **4** 1981
[11] Law M, Sirbuly D J, Johnson J C, Goldberger J, Saykally R J and Yang P 2004 *Science* **305** 1269
[12] Neumann U, Grunwald R, Griebner U, Steinmeyer G and Seeber W 2004 *Appl. Phys. Lett.* **82** 170
[13] Larciprete M C, Haertle D, Belardini A, Bertolotti M, Sarto F and Günter P 2006 *Appl. Phys.* B **82** 431
[14] Liu C Y, Zhang B P, Binh N T and Segawa Y 2004 *Appl. Phys.* B **79** 83
[15] Liu C Y, Zhang B P, Binh N T and Segawa Y 2004 *Opt. Commun.* **237** 65
[16] Neumann U, Grunwald R, Griebner U, Steinmeyer G, Schmidbauer M and Seeber W 2005 *Appl. Phys. Lett.* **87** 171108
[17] Zhang C F, Dong Z W, You G J, Zhu R Y, Qian S X, Deng H, Cheng H and Wang J C 2006 *Appl. Phys. Lett.* **89** 042117
[18] v Vugt L K, Rühle S, Ravindran P, Gerritsen H C, Kuipers L and Vanmaekelbergh D 2006 *Phys. Rev. Lett.* **97** 147401
[19] Konjhodzic D, Bretinger H, Wilczok U, Dreier A, Ladenburger A, Schmidt M, Eich M and Marlow F 2005 *Appl. Phys.* A **81** 425
[20] Schmidt M, Boettger G, Eich M, Morgenroth W, Huebner U, Meyer H G, Konjhodzic D, Bretinger H and Marlow F 2004 *Appl. Phys. Lett.* **85** 16
[21] Voss T, Svacha G T, Mazur E, Müller S, Ronning C, Konjhodzic D and Marlow F 2007 *Nano Lett.* **7** 3675
[22] Klingshirn C F 2005 *Semiconductor Optics* 2nd edn (Berlin: Springer)
[23] Yu P Y and Cardona M 2001 *Fundamentals of Semiconductors* 3rd edn (Berlin: Springer)
[24] Hauschild R, Priller H, Decker M, Brückner J, Kalt H and Klingshirn C 2006 *Phys. Status Solidi* c **3** 976
[25] Mingo N and Broido D A 2004 *Phys. Rev. Lett.* **93** 246106
[26] Madelung O 1999 *Landolt-Börnstein: II–VI and I–VII Compounds; Semimagnetic Compounds* (Heidelberg: Springer)
[27] Wischmeier L, Bekeny C and Voss T 2006 *Nonequilibrium Carrier Dynamics in Semiconductor* (*Springer Proceedings in Physics Series* vol 110) ed M Saraniti and U Ravaioli (Berlin: Springer) 261